DOI: 10.1002/ejic.200900288

Mixed-Ligand Complexes of Technetium and Rhenium with Tridentate Benzamidines and Bidentate Benzoylthioureas

Hung Huy Nguyen,[a][‡] Victor M. Deflon,[b] and Ulrich Abram*[c]

Keywords: Technetium / Rhenium / Structure elucidation / S,N,O ligands / S,O ligands / Synthetic methods

Mixed-ligand complexes of technetium(V) or rhenium(V) containing tridentate *N*-[(dialkylamino)(thiocarbonyl)]benzamidine (H_2L^1) and bidentate *N*,*N*-dialkyl-*N*′-benzoylthiourea (HL^2) ligands were formed in high yields when $(NBu_4)[MOCl_4]$ (M = Tc or Re) or $[ReOCl_3(PPh_3)_2]$ was treated with mixtures of the proligands. Other approaches for the synthesis of the products are reactions of $[MOCl(L^1)]$ complexes with HL^2 or compounds of the composition $[ReOCl_2(PPh_3)(L^2)]$ with H_2L^1. The resulting air-stable $[MO(L^1)(L^2)]$ complexes possess potential for the development of metal-based radiopharmaceuticals. $[TcO(L^1)(L^2)]$ complexes are readily reduced by PPh_3 with formation of $[Tc(L^1)(L^2)(PPh_3)]$. The resulting Tc^{III} complexes undergo two almost-reversible oxidation steps corresponding to one-electron transfer processes.

(© Wiley-VCH Verlag GmbH & Co. KGaA, 69451 Weinheim, Germany, 2009)

Introduction

The coordination chemistry of technetium and rhenium has constantly been attended due to both the widespread use of the radionuclide ^{99m}Tc in diagnostic nuclear medicine and the potential of the β-emitting radioisotopes ^{186}Re and ^{188}Re in radiotherapy.[1,2] In this context, there is a continuous need for efficient chelating systems. Ligands that are suitable for the stabilization of the $\{M^V{=}O\}^{3+}$ cores (M = Re, Tc) are of particular interest, as reduction of $[MO_4]^-$ ions from the commercial generator systems with common reducing agents frequently form oxidometallates(V). Ligand systems that form such complexes of sufficient stability under physiological conditions are tetradentate N,S,O chelators.[3,4] However, the tuning of the biological properties of the resulting complexes by variations in the periphery of the ligands is difficult and sometime results in the formation of different stereoisomers.[4] Mixed-ligand approaches give access to a smooth tuning of the ligand properties and, thus, of their biological behaviour.

Following the so-called mixed-ligand concept, many "3+1" systems, which are neutral complexes with a $[MO]^{3+}$ core and a mixed-ligand set of a dianionic tridentate ligand containing one or more sulfur donor atoms, such as, [SSS], [SOS], [SNS], [SNN] or [ONS] and a monodentate thiolate, were studied.[5] Finally, it was found that many of these "3+1" complexes were relatively unstable in vitro and in vivo as a result of ready substitution of the labile monothiolate RS^- by physiological thiols such as cysteine or glutathione.[6] Generally, this can be explained by the 16 valence electron nature of the 5-coordinate "3+1" complexes. Replacement of the labile monothiolate by bidentate ligands results in so-called "3+2" systems with a closed-shell electron configuration and a higher stability is expected.[7] Thus, several "3+2" mixed-ligand complexes with ligands carrying different donor sets such as [SNS]/[PO],[7] [NOS]/[NO],[8] [NOS]/[NN],[9] [NON]/[OO],[10] [NOS]/[SN][11] or [ONO]/[PO] were studied.[12] Some of them show interesting properties, which encourages further studies and the introduction of hitherto unexplored ligand systems in such considerations.

In previous papers, we described a new class of tridentate *N*-[(dialkylamino)(thiocarbonyl)]benzamidine ligands (H_2L^1) that form stable, five-coordinate complexes of the composition $[ReOCl(L^1)]$ (**1**)[13] and elucidated the coordination chemistry of *N*,*N*-dialkyl-*N*′-benzoylthioureas (HL^2) with rhenium and technetium.[14] The advantage of these two ligand classes is the convenience of modification in the periphery of their chelating system. This allows variation of the basis properties of the products such as solubility, polarity and lipophilicity and also gives access to bioconjugation through the periphery of the tridentate ligands. With

[a] Department of Chemistry, Hanoi University of Sciences, 19 Le Thanh Tong, Hanoi, Vietnam
[b] Instituto de Química de São Carlos, Universidade de São Paulo, 13566-590 São Carlos – SP, Brazil
[c] Institute of Chemistry and Biochemistry, Freie Universität Berlin, Fabeckstr. 34/36, 14195 Berlin, Germany
Fax: +49-30-838-52676
E-mail: abram@chemie.fu-berlin.de
[‡] Present address: Institute of Chemistry and Biochemistry, Freie Universität Berlin, Fabeckstr. 34/36, 14195 Berlin, Germany
Supporting information for this article is available on the WWW under http://dx.doi.org/10.1002/ejic.200900288.

 © 2009 Wiley-VCH Verlag GmbH & Co. KGaA, Weinheim

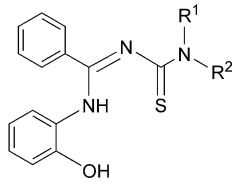

H_2L^1

H_2L^{1a}: $R^1 = R^2$ = Et
H_2L^{1b}: R^1, R^2 = Morph

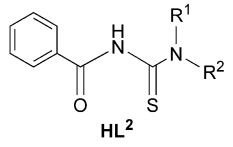

HL^2

HL^{2a}: $R^1 = R^2$ = Ph
HL^{2b}: R^1, R^2 = Morph

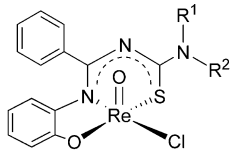

1

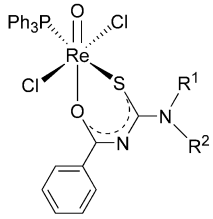

2

complexes of types **1** and **2**, appropriate starting materials are available with the bidentate and tridentate ligands already in coordination positions, which are expected for the intended mixed-ligand compounds.

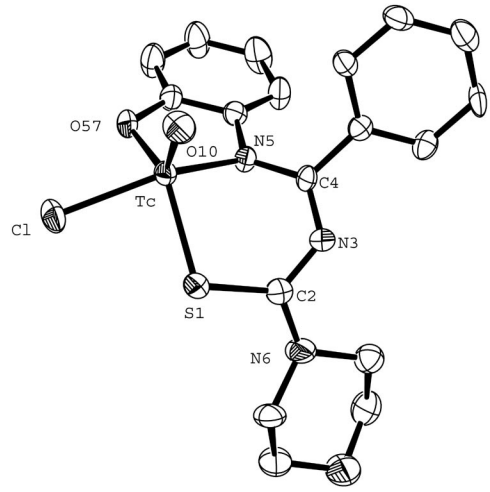

Figure 1. Ellipsoid representation of the molecular structure of **3**.[5] Thermal ellipsoids represent 50% probability. H atoms are omitted for clarity.

Table 1. Selected bond lengths [Å] and angles [°] in **3**.

Tc–O10	1.641(4)	S1–C2	1.764(6)
Tc–Cl	2.3479(14)	C2–N3	1.336(7)
Tc–S1	2.3011(12)	N3–C4	1.305(6)
Tc–N5	2.001(4)	C4–N5	1.365(6)
Tc–O57	1.951(3)	C2–N6	1.315(7)
O10–Tc–Cl	105.86(15)	O10–Tc–N5	105.46(19)
O10–Tc–S1	109.35(14)	O10–Tc–O57	115.06(18)

Results and Discussion

$(NBu_4)[TcOCl_4]$ reacts with an equivalent amount of H_2L^{1b} in methanol with formation of the complex $[TcOCl(L^{1b})]$ (**3**). The product precipitates almost quantitatively as a red, microcrystalline solid directly from the reaction mixture. The addition of a supporting base is not required.

The IR spectrum of **3** exhibits a $\nu_{Tc=O}$ frequency at 972 cm^{-1} and indicates a strong bathochromic shift of the C=N band as a consequence of the formation of the complex. The ^1H NMR spectrum provides additional evidence for the proposed composition of the compound. The complex pattern of the protons in the morpholinyl residue indicates a hindered rotation around the C–$N(CH_2)_4O$ bond. This is not surprising and has been observed previously for the uncoordinated benzamidine as well as for the corresponding oxidorhenium(V) complex.[13]

Figure 1 shows the molecular structure of **3** and selected bond lengths and angles are given in Table 1. The technetium atom possesses a distorted square-pyramidal coordination environment with the oxido ligand in the apical position. The basal plane is defined by the donor atoms of the tridentate ligand and the chlorido ligand. The Tc atom is situated 0.689(2) Å above this plane towards the oxido ligand. All O10–Tc–X angles (X = equatorial donor atom) fall in the range between 105 and 115°. This corresponds with the typical bonding situation of square-pyramidal Tc^VO complexes.[15] The Tc=O distance of 1.641(4) Å is within the expected range for a technetium–oxygen double bond.[16]

The mixed-ligand complexes $[MO(L^1)(L^2)]$ (M = Tc, Re) can be synthesized by four alternative routes (Scheme 1). The first approach (path A) is a two-step synthesis using $[MO(L^1)Cl]$ (**1**) compounds as intermediate complexes. The labile square-pyramidal complexes are subsequently treated with equivalent amounts of the benzoylthioureas in warm CH_2Cl_2/MeOH. The mixed-ligands complexes are formed in high yields following this procedure. They are readily soluble in CH_2Cl_2 and only sparingly soluble in MeOH. Single crystals of good quality were obtained by slow evaporation of the reaction mixtures.

The second two-step synthesis (path B) starts from a common precursor, $[ReOCl_3(PPh_3)_2]$. In the first step, $[ReOCl_3(PPh_3)_2]$ is treated with a slight excess of the corresponding benzoylthiourea in CH_2Cl_2 to give monosubstituted complexes of the composition $[ReOCl_2(L^2)(PPh_3)]$ (**2**).[14a] In the last step, compounds **2** are exposed to equivalent amounts of H_2L^1 in refluxing CH_2Cl_2 until the initial green-yellow colour changes to clear red. The yields of analytically pure mixed-ligand complexes from this synthetic approach are significantly lower than those using $[ReO(L^1)Cl]$ as starting materials. This is most probably the result of incomplete substitution and/or further reduction of the $\{ReO\}^{3+}$ core by released PPh_3 under the conditions applied. Such side reactions, which finally yield rhenium(III) complexes, are common when phosphanes are present.[17]

The mixed complexes can be also prepared in good yield in one-pot reactions starting from $(NBu_4)[ReOCl_4]$ or $[ReOCl_3(PPh_3)_2]$ and stoichiometric amounts of the tri-

 © 2009 Wiley-VCH Verlag GmbH & Co. KGaA, Weinheim

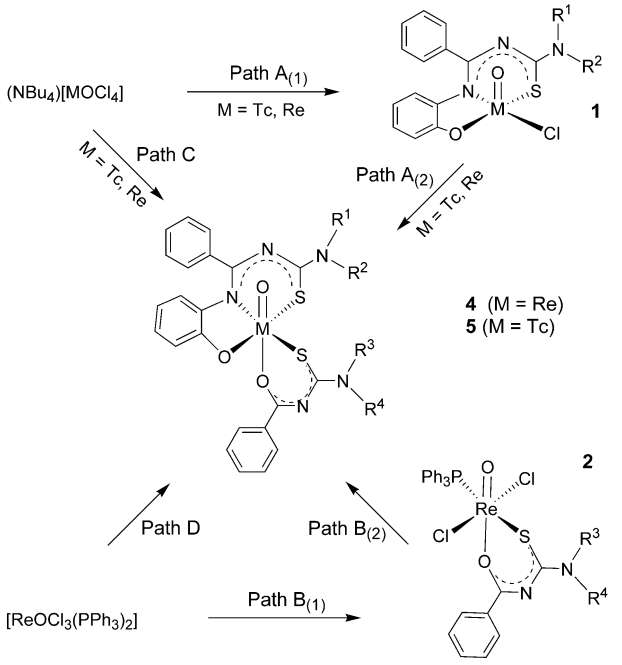

Scheme 1. Synthetic approaches for the "3+2" mixed-ligand complexes under study. Path A: (1) H_2L^1, MeOH, room temp.; (2) HL^2, Et_3N, CH_2Cl_2/MeOH, 35 °C. Path B: (1) HL^2, CH_2Cl_2, room temp.; (2), H_2L^1, Et_3N, CH_2Cl_2, reflux. Path C: H_2L^1, HL^2, Et_3N, CH_2Cl_2/MeOH, 35 °C. Path D: H_2L^1, HL^2, Et_3N, CH_2Cl_2, room temp.

dentate benzamidines and benzoylthioureas. Reactions starting from $(NBu_4)[ReOCl_4]$ (path C) are best done in CH_2Cl_2/MeOH mixtures, whereas CH_2Cl_2 should be used for reactions starting from $[ReOCl_3(PPh_3)_2]$ (path D). The yields of such reactions are not significantly lower than those following path A. However, the supporting base NEt_3 should be added in such reactions a few minutes after the addition of the ligands in order to complete the reaction and to avoid rapid hydrolysis of the precursors.

Infrared spectra of oxidorhenium mixed-ligands complexes **4** show no absorptions in the region above 3100 cm^{-1}, which correspond to ν_{NH} and ν_{OH} vibrations in uncoordinated H_2L^1 and HL^2 and indicate the expected double deprotonation of the benzamidines and deprotonation of benzoylthioureas during the formation of the complexes. Additionally, the sharp intense absorptions in the range between 1620–1690 cm^{-1} assigned to the $\nu_{C=N}$ and $\nu_{C=O}$ stretches in the spectra of the noncoordinated benzamidines and thioureas shift to the range between 1500 and 1540 cm^{-1} and appear as broad bands. An unambiguous assignment of the two bands either to the thiocarbamoylbenzamidine or benzoylthiourea stretches have not been done. Despite the fact that these absorptions are about 30 cm^{-1} higher than the corresponding bands in the infrared spectra of both **1** and **2**, the bathochromic shifts of about 100 cm^{-1} with respect to H_2L^1 and HL^2 indicate for both ligands the formation of a chelate with a large degree of π-electron delocalization within the chelate rings. Intense bands appear between 964 and 980 cm^{-1}, which can be assigned to the Re=O stretches.[17]

The NMR spectra of complexes **4** provide additional evidence for the proposed composition and the molecular structures of the complexes. The hindered rotation around the C–NR_2 bonds results in magnetic inequivalence of the two residues R. Thus, two triplet signals of the methyl groups in the –NEt_2 residue are observed in the ^1H NMR spectrum of $[ReO(L^{1a})(L^{2a})]$ (**4a**) measured at room temperature. However, the proton signals of the two methylene groups, which should consequently be two quartet signals, appear as four sextet resonances with an ABX_3 coupling pattern, where J_{AB} is approximately twice the value of J_{AX} including two overlapping signals at 3.79 ppm and two well-separated signals at 3.97 and 4.05 ppm. This splitting pattern of the methylene signals can be explained by the rigid structure of the tertiary amine group, which makes the methylene protons magnetically inequivalent with respect to their axial and equatorial positions. More interestingly, the ^1H NMR spectrum of $[ReO(L^{1a})(L^{2b})]$ (**4b**) shows the rigidity for the whole morpholinyl moiety of $\{L^{2b}\}^-$, which results in eight magnetically inequivalent protons in this unit. This is indicated by five well-resolved multiplet signals with ABXY splitting model at 4.02, 4.20, 4.37, 4.42, 4.62 ppm corresponding to four different CH_2–O protons and one CH_2–N proton. Three other CH_2–N protons appear together with two CH_2–N protons of the NEt_2 residue of $\{L^{1a}\}^{2-}$ as a broad multiplet at 4.00 ppm. A similar magnetic behaviour of the morpholinyl moieties, but less resolved, is observed in the ^1H NMR spectrum of $[ReO(L^{1b})(L^{2b})]$ (**4c**). The ^{13}C NMR spectra of the complexes are easier to explain, as their patterns are only influenced by hindered rotation around the C–NR_2 bonds. Consequently, two separated signals for each CH_2 and CH_3 carbon atom in the NEt_2 groups and/or CH_2–N and CH_2–O atoms in the morpholinyl units appear. The chemical shifts of the aromatic carbon atoms, which cannot be unambiguously assigned, are in the range from 117–136 ppm, with the exception of the C_{ar}–N and C_{ar}–O resonances, which clearly appear in the lower field regions at 145 and 165 ppm, respectively. This is due to deprotonation of the imino and phenol groups during the complex formation of the H_2L^1 ligands. The low-intensity resonances of the carbon atoms of the C=X (X = N, O, S) groups are in the range from 163 to 187 ppm. The closely related structures of the benzoylthioureas and thiocarbamoylbenzamidines produce some difficulties in the assignment of the C=X signals in the ^{13}C NMR spectra of complexes **4**. Nevertheless, with regard to the analogous coordination spheres of **4a** and **4b**, the chemical shifts of the C=X signals of $\{L^{1a}\}^{2-}$ in these complexes should be similar. Thus, the comparison of the chemical shift values give hints for a detailed assignment of the C=X signals (see Experimental Section). Although the chemical shift values of the C=S resonances of the benzoylthiourea ligands in the mixed-ligand complexes are in the same range as those of precursors **2**, the corresponding C=O resonances are shifted to higher field by about 5 ppm. Both C=N and C=S resonances of the $\{L^1\}^{2-}$ ligand appear at lower field by about 6 ppm compared with the values in the spectra of **1**.[13]

 © 2009 Wiley-VCH Verlag GmbH & Co. KGaA, Weinheim

The mass spectra (FAB^+) of the mixed-ligand complexes show intense peaks of the molecular ions with the expected isotopic patterns. Interestingly, the fragments that result from the loss of the $R^3R^4NC{\equiv}N$ residues from the benzoylthiourea ligands appear in all spectra as high intensity signals. The complete loss of the $\{L^2\}^-$ ligands is also observed in the mass spectra of all complexes of type **4**.

The structures of complexes **4a** and **4b** were studied by X-ray diffraction. As a representative for this type of complex, the molecular structure of **4a** is shown in Figure 2. Because the structure of **4b** is identical with the exception of the residues of the benzoylthiourea ligand, no extra figure is shown. Table 2 contains selected bond lengths and angles for both compounds. In both complexes, the rhenium atoms possess a distorted octahedral coordination environment. Axial positions are occupied by the oxido ligands and the oxygen atoms of the bidentate ligands. The tridentate benzamidine ligands occupy three positions in the equatorial coordination sphere, which is completed by the sulfur atoms of $\{L^2\}^-$. The metal atoms are located slightly above the mean least-square plane formed by S1, N5, O57 and S12 toward the oxido ligand. The Re=O distances of 1.662(4) and 1.681(2) Å are in the expected range of rhenium–oxygen double bonds.[17]

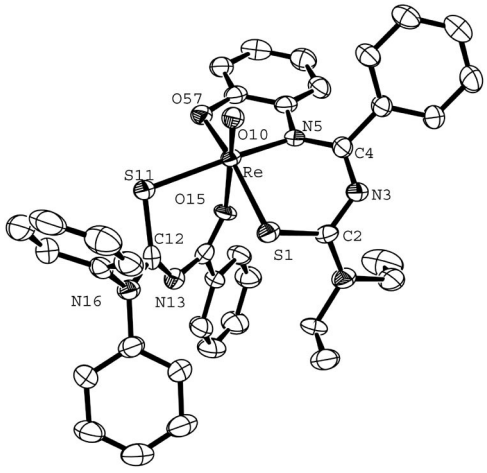

Figure 2. Ellipsoid representation of the molecular structure of **4a**.[25] Thermal ellipsoids represent 50% probability. H atoms are omitted for clarity.

A remarkable structural feature is the coordination of the benzoylic oxygen atoms *trans* to the oxido ligand. The Re1–O15 bonds fall in the range from 2.158(2) to 2.196(4) Å. This is significantly longer than the corresponding Re–O bonds in complexes **2**, whereas the corresponding C14–O15 bonds are only shorter than those in complexes **2** with the same benzoylthioureas by about 0.03 Å.[13] The Re–O15 bong lengths in **4** are at the upper limit of *trans*-O=Re–O single bond lengths in Re^V oxido complexes. Similar values have previously only been reported for some complexes with small monodentate neutral ligands such as H_2O, MeOH or Me_2CO.[17] This means that an electron transfer from the Re=O double bond to a *trans*-Re–O single bond, which is frequently observed for alkoxido-type ligands, does not apply for the compounds under study.[18]

Table 2. Selected bond lengths [Å] and angles [°] in **4a**, **4b** and **5**.

	4a	**4b**	**5**
M–O10	1.662(4)	1.681(2)	1.641(4)
M–S1	2.360(2)	2.354(1)	2.344(2)
M–N5	2.009(6)	2.028(2)	2.048(4)
M–O57	1.988(5)	1.996(2)	1.998(4)
M–O15	2.196(4)	2.158(2)	2.200(4)
M–S11	2.399(2)	2.408(1)	2.414(1)
S1–C2	1.741(7)	1.748(2)	1.748(6)
S11–C12	1.754(8)	1.750(3)	1.749(6)
C2–N3	1.348(9)	1.342(3)	1.323(7)
C12–N13	1.335(9)	1.343(3)	1.333(7)
N3–C4	1.298(9)	1.311(3)	1.308(7)
N13–C14	1.346(9)	1.335(3)	1.333(7)
C4–N5	1.367(9)	1.355(3)	1.357(8)
C14–O15	1.252(8)	1.261(3)	1.268(6)
C2–N6	1.328(8)	1.331(3)	1.338(8)
C12–N16	1.340(9)	1.334(3)	1.342(7)
O10–M–S1	96.4(2)	94.5(1)	100.0(2)
O10–M–S11	97.2(2)	99.0(1)	96.9(1)
O10–M–N5	101.5(2)	103.0(1)	103.4(2)
O10–M–O57	103.8(2)	102.6(1)	99.3(2)
O10–M–O15	175.0(2)	176.5(1)	176.5(2)
O57–M–N5	80.4(2)	80.5(1)	81.8(2)
O57–M–S1	159.8(1)	162.9(1)	160.7(1)
O57–M–S11	86.1(1)	86.3(1)	90.9(1)
O57–M–O15	79.4(2)	80.4(1)	79.7(2)
N5–M–S1	95.0(2)	96.7(1)	93.7(1)
N5–M–S11	159.1(2)	156.3(1)	159.3(1)
N5–M–O15	82.7(2)	79.3(1)	79.8(2)
S1 –M–S11	92.1(1)	90.1(1)	86.86(6)
S1 –M–O15	80.5(1)	82.5(1)	81.1(1)
S11–M–O15	79.1(1)	79.2(1)	79.9(1)

The Re–S11 and C12–S11 bond lengths are in the typical range of Re–S single bonds and C–S bonds with partial double-bond character, as has been reported for other benzoylthiourea complexes of rhenium previously.[14] In the benzamidine moiety, the Re–S1 and Re–N5 bond lengths are lengthened by about 0.03–0.06 Å with respect to the bonds in complexes **1**.[13] Nevertheless, the Re–S1 bond lengths are still about 0.06 Å shorter than the Re–S11 bonds in the co-coordinated benzoylthiourea ligands. The atoms S11, C12, N13, C14 and O15 lie almost in a plane with a maximum deviation from a mean least-square plane of only 0.175(5) Å for C12 in **4a** and 0.097(2) Å for C14 in **4b**. The six-membered chelate rings, however, which are formed from these atoms and the Re atoms, are dramatically distorted with distances of metal atoms to mean least-square plane of 1.157(7) and 1.093(3) Å for **4a** and **4b**, respectively. The six-membered chelate rings of the ligands $\{L^1\}^{2-}$ are only slightly distorted with maximum deviations from a mean least-square plane of about 0.30 Å. A considerable delocalization of π-electron density is found inside all chelate rings. This is indicated by similar lengths of all C–N bonds, which fall within the range between C–N single and double bonds. These bond length equalizations are also extended to the C2–N6/C12–N16 bonds (1.33–1.34 Å). The

 © 2009 Wiley-VCH Verlag GmbH & Co. KGaA, Weinheim

partial transfer of electron density into these bonds agrees well with the ^{1}H NMR spectra of the compounds, which indicates a rigid arrangement of –NR^1R^2 moiety.

The synthetic approaches to the mixed-ligand complexes outlined in paths B and D (Scheme 1) are restricted to rhenium, as a compound of the composition "[$TcOCl_3(PPh_3)_2$]" does not exist due to the ready reduction of technetium by phosphanes with formation of Tc^{IV} and Tc^{III} compounds. We were consequently also not able to prepare a complex of the composition "[$TcOCl_2(L^2)(PPh_3)$]". Nevertheless, we succeeded in the synthesis of the corresponding technetium mixed-ligand complexes (Schemes 1 and 2) following the approaches in paths A and C. Figure 3 shows the molecular structure of one of these complexes, [$TcO(L^{1b})(L^{2b})$] (**5**), which was isolated as a green crystalline solid in high yields from both synthetic pathways.

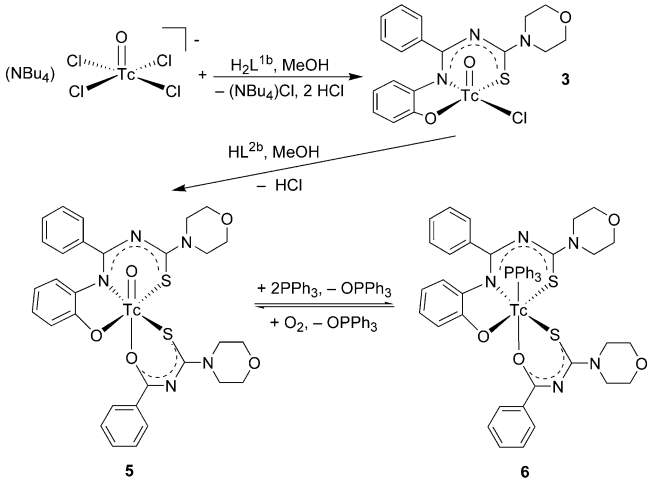

Scheme 2. Formation and reactions of the technetium mixed-ligand compounds.

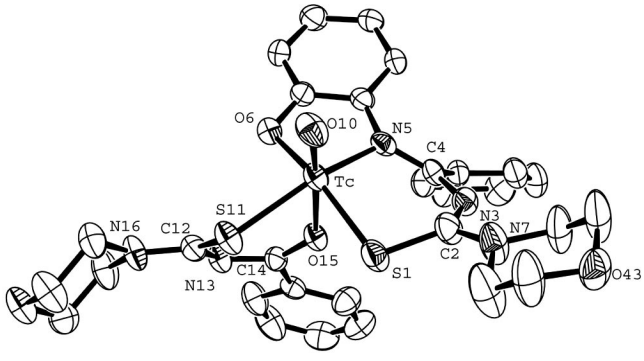

Figure 3. Ellipsoid representation of the molecular structure of **5**.[25] Thermal ellipsoids represent 50% probability. H atoms are omitted for clarity.

The IR spectrum of **5** exhibits the $\nu_{Tc=O}$ frequency at 957 cm^{-1}, and the spectral features described above for compounds **4**, such as the strong bathochromic shift of the C=O and C=N bands, also apply for the Tc complex. The presence of two rigid morpholinyl residues in the molecule leads to a complicated pattern of the methylene region of the ^{1}H NMR spectrum of **5**. However, three multiplet signals of three CH_2–O protons with a typical ABXY splitting pattern can clearly be resolved at 4.35, 4.53 and 4.75 ppm.

All main structural features of compound **5** are similar to the facts discussed for complexes **4** and shall not be repeated here in detail. The corresponding bond lengths and angles are compared to those of the structurally characterized rhenium mixed-ligand complexes in Table 2. However, the orientation of the tridentate ligand is different from those observed in the analogous rhenium compounds. This can easily be seen at the phenyl ring at the C4 atom. It is directed away from the oxido ligand in **5**, whereas it is positioned above the equatorial coordination plane in complexes **4a** and **4b**, which is probably caused by the fluctuation of the whole molecule.

Compound **5** readily reacts with an excess amount of PPh_3 in CH_2Cl_2 with formation of a red crystalline technetium(III) complex of the composition [$Tc(PPh_3)(L^{1b})(L^{2b})$] (**6**). This reaction proceeds in high yields even at room temperature, but it should be mentioned that similar reactions with the corresponding rhenium complexes **4** could not be observed. The reduction of oxidotechnetium(V) complexes by phosphanes is not uncommon and can be explained by the formation of an intermediate $\{Tc–OPPh_3\}^{3+}$ complex, and the subsequent abstraction of $OPPh_3$ from the coordination sphere.[14a] Indeed, released $OPPh_3$ could be detected by ^{31}P NMR spectroscopic analysis of the reaction mixture between **5** and PPh_3. The resulting technetium(III) product is stable as a solid, whereas in solution slow oxidation by air was observed. It is accompanied by a change in the colour from red to yellow-green. Recrystallization of **6** from a CH_2Cl_2/MeOH mixture must be performed under anaerobic conditions or in the presence of an extra amount of PPh_3 to avoid ongoing oxidation.

The infrared spectrum of complex **6** confirms the reduction of the metal atom by the absence of a typical $\nu_{Tc=O}$ stretch between 900 and 1000 cm^{-1}. The $\nu_{C=O}$ and/or $\nu_{C=N}$ bands are slightly shifted to longer wavelengths compared to **5** and appear at 1497 cm^{-1} as a strong broad band.

Figure 4 shows the molecular structure of **6**. Selected bond lengths and angles are contained in Table 3. The coordination environment of the metal atom is best described as a distorted octahedron with *trans* angles between 168.4(3) and 178.8(3)°. The ligand $\{L^{2b}\}^-$ coordinates to technetium as a common S,O bidentate ligand with its oxygen atom *trans* to the PPh_3 ligand. The three remaining positions in the coordination sphere are occupied by the planar tridentate $(L^{1b})^{2-}$ ligand. The Tc–O15 bond length of 2.072(9) Å falls in the range of typical Tc–O single bonds. The Tc–S1 and Tc–S11 bond lengths are almost equal and in the same range as those of other Tc^{III} benzoylthioureato complexes such as [$TcCl(PPh_3)(L^{2a})_2$] and [$Tc(L^{2a})_3$].[14]

The redox behaviour of **6** as described above reveals some interesting features, which encouraged us to study its electrochemistry. Thus, the cyclic voltammetry measurement of the compound was undertaken in dry CH_2Cl_2 under an argon atmosphere. Complex **6** shows no reduction process from –1.2 to 0.0 V, but two almost-reversible oxi-

 © 2009 Wiley-VCH Verlag GmbH & Co. KGaA, Weinheim

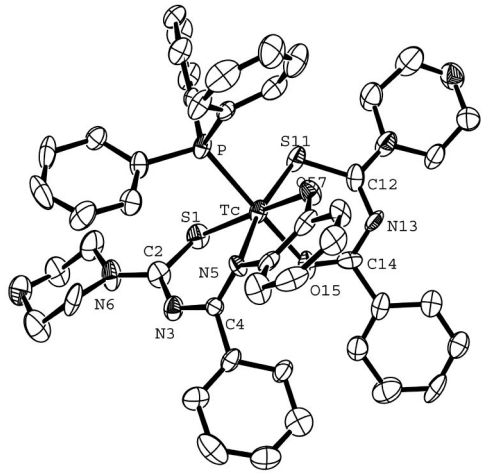

Figure 4. Ellipsoid representation of the molecular structure of **6**.[25] Thermal ellipsoids represent 40% probability. H atoms are omitted for clarity.

Table 3. Selected bond lengths [Å] and angles [°] in **6**.

Tc–P	2.413(4)	S1–C2/S11–C12	1.75(1)/1.74(1)
Tc–S1	2.346(4)	C2–N3/C12–N13	1.34(1)/1.33(1)
Tc–N5	2.09(1)	N3–C4/N13–C14	1.37(1)/1.34(1)
Tc–O57	2.048(8)	C4–N5/C14–O15	1.28(2)/1.26(1)
Tc–O15	2.072(9)	C2–N6/C12–N16	1.36(1)/1.37(2)
Tc–S11	2.341(4)		
O10–Tc–S1	87.3(1)	O57–Tc–O15	87.2(3)
O10–Tc–S11	91.0(1)	N5–Tc–S1	92.3(3)
O10–Tc–N5	97.4(3)	N5–Tc–S11	168.4(3)
O10–Tc–O57	91.8(3)	N5–Tc–O15	83.0(4)
O10–Tc–O15	178.8(3)	S1 –Tc–S11	96.0(1)
O57–Tc–N5	82.0(4)	S1 –Tc–O15	93.8(3)
O57–Tc–S1	174.0(3)	S11 –Tc–O15	88.4(3)
O57–Tc–S11	89.9(3)		

dations at 0.218 V (ΔE_p = 98 mV) and 1.078 V (ΔE_p = 85 mV) corresponding to one-electron transfer processes (Figure 5). It is necessary to note that under the same conditions the ΔE_p value of the Fc/Fc$^+$ couple is 83 mV. The low potential of the first oxidation process is in agreement with the observed oxidation of **6** under aerobic conditions. It is understood that on the timescale of the applied CV, the $[Tc^V(PPh_3)(L^{1b})(L^{2b})]^{2+}$ species is sufficiently kinetically inert to undergo the backward reduction. However, in the oxidation reaction of **6** in air, oxido complex **5** is the thermodynamically more stable product.

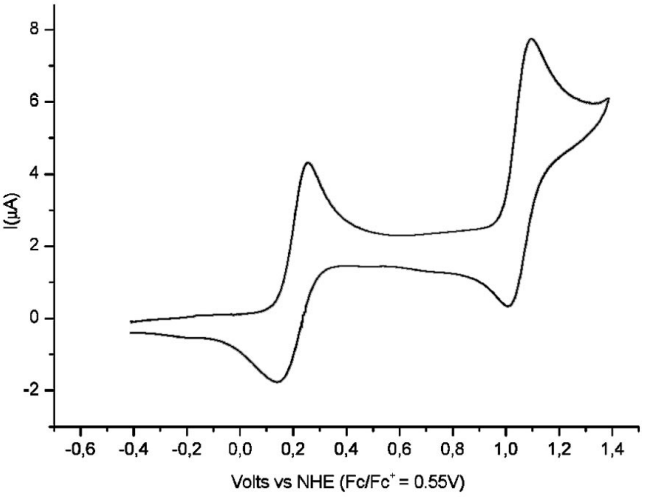

Figure 5. Cyclic voltammogram of **6** in 0.2 M $[NBu_4][PF_6]/CH_2Cl_2$ at a scan rate of 100 mV s^{-1}.

$$[Tc^{III}(PPh_3)(L^{1b})(L^{2b})] \underset{+e}{\overset{-e}{\rightleftharpoons}} [Tc^{IV}(PPh_3)(L^{1b})(L^{2b})]^+ \underset{+e}{\overset{-e}{\rightleftharpoons}} [Tc^{V}(PPh_3)(L^{1b})(L^{2b})]^{2+}$$

Conclusions

We could demonstrate that mixed-ligand complexes of technetium and rhenium containing tridentate *N*-[(dialkylamino)(thiocarbonyl)]benzamidine and bidentate *N*,*N*-dialkyl-*N*′-benzoylthiourea ligands are readily formed following different protocols. The mixed-ligand complexes represent the most stable species in solutions, which contain the common oxidorhenium(V) precursors $(NBu_4)[ReOCl_4]$ or $[ReOCl_3(PPh_3)_2]$ and mixtures of both chelating ligands.

The presented study on prototype compounds is the experimental basis of ongoing studies in our laboratory that deal with ligands of the same type, which contain anchor groups for the conjugation to peptides or proteins, for example, the benzamidine derivative H_2L^3.

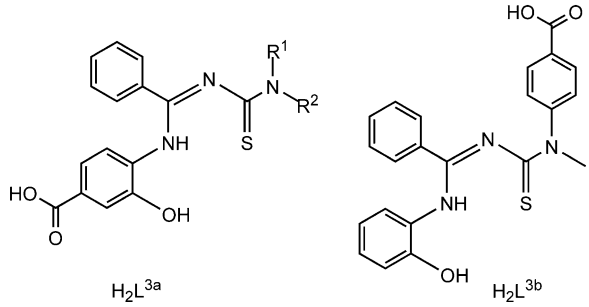

Experimental Section

Materials: All reagents used in this study were reagent grade and used without further purification. Solvents were dried and freshly distilled prior to use unless otherwise stated. $(NBu_4)[ReOCl_4]$, $(NBu_4)[TcOCl_4]$ and $[ReOCl_3(PPh_3)]$ were prepared by published methods.[19–21] H_2L^1 and HL^2 were synthesized by standard procedures.[13,22,23] The syntheses of the $[ReOCl(L^1)]$ (**1**) and $[ReOCl_2(L^2)(PPh_3)]$ (**2**) complexes are described in previous papers.[13,14]

Radiation Precautions: ^{99}Tc is a weak β$^-$-emitter. All manipulations with this isotope were performed in a laboratory approved for the handling of radioactive materials. Normal glassware provides adequate protection against the low-energy β emission of the technetium compounds. Secondary X-rays (bremsstrahlung) play an important role only when larger amounts of ^{99}Tc are used.

Physical Measurements: Infrared spectra were measured as KBr pellets with a Shimadzu FTIR spectrometer between 400 and 4000 cm^{-1}. Mass spectra (FAB$^+$) were recorded with a TSQ (Finni-

 © 2009 Wiley-VCH Verlag GmbH & Co. KGaA, Weinheim

gan) instrument by using a nitrobenzyl alcohol matrix or the spectra (ESI^+) were measured with an Agilent 6210 ESI-TOF (Agilent Technologies). Elemental analysis of carbon, hydrogen, nitrogen and sulfur were determined by using a Heraeus vario EL elemental analyzer. The ^{99}Tc values were determined by standard liquid scintillation counting. NMR spectra were recorded with a JEOL 400 MHz multinuclear spectrometer. Cyclic voltammetry measurements were performed with a PCI4 (Gamry Instruments) by using a conventional three-electrode cell with working and counter platinum wire electrodes and an Ag wire pseudoelectrode. The measurements were carried out in CH_2Cl_2 solutions with a scan rate of 0.1 $V s^{-1}$ at T = 293 K with [nBu$_4$N][PF_6] as supporting electrolyte. Potentials were quoted relative to the Fc/Fc^+ couple used as internal reference ($E_{1/2}$ = 0.55 V vs. SCE).

[TcO(L^{1b})Cl] (3): H_2L^{1b} (34 mg, 0.1 mmol) dissolved in MeOH (3 mL) was added dropwise to a stirred solution of (NBu_4)[$TcOCl_4$] (50 mg, 0.1 mmol) in MeOH (2 mL). The colour of the solution immediately turned deep red and a red precipitate deposited within a few minutes. The red powder was filtered off and washed with cold methanol. X-ray quality single crystals of **3** were obtained by slow evaporation of a CH_2Cl_2/acetone solution. Yield: 88% (43 mg). $C_{18}H_{17}ClN_3O_3STc$ (473.77): calcd. Tc 20.2; found Tc 20.1. IR (KBr): $\tilde{\nu}$ = 3051 (w), 2970 (w), 2916 (w), 2851 (w), 1520 (vs), 1470 (vs), 1439 (vs), 1352 (s), 1311 (m) 1265(s), 1246 (vs), 1175 (w), 1115 (s), 1026 (s), 972 (s), 771 (m), 741 (m), 691 (m), 672 (m) cm^{-1}. ^1H NMR (400 MHz, $CDCl_3$): δ = 3.7–4.0 (m, 4 H, N-CH_2), 4.2–4.4 (m, 4 H, O-CH_2), 6.56 (t, J = 7.8 Hz, 1 H, PhOH), 6.61 (d, J = 7.0 Hz, 1 H, PhOH), 6.93 (t, J = 6.6 Hz, 1 H, PhOH), 7.32 (d, J = 7.6 Hz, 1 H, PhOH), 7.43 (t, J = 7.8 Hz, 2 H, Ph), 7.55 (t, J = 7.4 Hz, 1 H, Ph), 7.73 (d, J = 7.3 Hz, 2 H, Ph) ppm.

[ReO(L^1)(L^2)] (4)

Path A: To a solution of [ReO(L^1)Cl] (0.1 mmol) in CH_2Cl_2 (5 mL) was added HL^2 (0.1 mmol) and NEt_3 (3 drops). The red-coloured solution was stirred at 35 °C for 2 h, and the solvent was removed in vacuo. The resulting residue was either washed with cold MeOH or recrystallized from CH_2Cl_2/MeOH to give a red crystalline product. Yield: 70–90%

Path B: To a solution of [$ReOCl_2$(L^2)(PPh_3)] (0.1 mmol) in CH_2Cl_2 (5 mL) was added H_2L^1 (0.1 mmol) in CH_2Cl_2 (3 mL) and Et_3N (3 drops). The mixture was heated at reflux for 3 h, whereupon the colour changed from green-yellow to deep red. The solvent was removed under reduced pressure, and the residue was treated as described for path A. Yield: 30–53%

Path C: To a solution of (NBu_4)[$ReOCl_4$] (58 mg, 0.1 mmol) in CH_2Cl_2 (3 mL) was added a mixture of H_2L^1 (0.1 mmol) and HL^2 (0.1 mmol) in MeOH (3 mL). After stirring at room temperature for 15 min, NEt_3 (3 drops) was added, and the mixture was stirred at 35 °C for 2 h. This resulted in the formation of a dark-red solution. The solvent was removed under reduced pressure, and the resulting residue was treated as described for path A. Yield: 72–85%.

Path D: To a suspension of [$ReOCl_3(PPh_3)_2$] (83 mg, 0.1 mmol) in CH_2Cl_2 (3 mL) was added a mixture of H_2L^1 (0.1 mmol) and HL^2 (0.1 mmol) in CH_2Cl_2 (3 mL). After stirring at room temperature for 15 min, the sparingly soluble rhenium complex was dissolved and a clear solution was formed, the colour of which slowly turned to red. The addition of NEt_3 (3 drops) resulted in an immediate change of the colour and a deep red solution was obtained within a few seconds. The solvent was removed under reduced pressure, and the resulting residue was treated as described for path A. Yield: 67–81%.

[ReO(L^{1a})(L^{2a})] (4a): $C_{38}H_{34}N_5O_3ReS_2$ (859.05): calcd. C 53.13, H 3.99, N 8.15, S 7.47; found C 53.02, H 4.07, N 8.01, S 7.67. IR (KBr): $\tilde{\nu}$ = 3051 (w), 2978 (w), 2923 (w), 1539 (vs), 1473 (vs), 1414 (vs), 1357 (s), 1250 (vs), 1172 (w), 1141 (w), 1026 (w), 980 (s), 748 (m), 698 (m) cm^{-1}. ^1H NMR (400 MHz, $CDCl_3$): δ = 1.32 (t, 6 H, CH_3), 3.80 (m, 2 H, CH_2), 3.97 (m, 1 H, CH_2), 4.05 (m, 1 H, CH_2), 6.25 (t, J = 7.6 Hz, 1 H, PhOH), 6.38 (d, J = 6.5 Hz, 1 H, PhOH), 6.72 (t, J = 7.7 Hz, 1 H, PhOH), 6.91 (t, J = 7.8 Hz, 2 H, Ph), 7.01 (d, J = 6.8 Hz, 1 H, PhOH), 7.1–7.7 (m, 18 H, Ph) ppm. ^{13}C NMR (100 MHz, $CDCl_3$): δ = 13.44 (CH_3), 13.51 (CH_3), 47.17 (CH_2), 47.20 (CH_2), 117–135 (Ph + PhOH) 145.30 (C_{ar}–N), 163.67 (C_{ar}–O), 171.46 (C=N, {L^{1a}}$^{2-}$), 173.02 (C=S, {L^{2a}}$^-$), 179.24 (C=S, {L^{1a}}$^{2-}$), 187.97 (C=O, {L^{2a}}$^-$) ppm. MS (FAB+): m/z (%) = 882 (6) [M + Na]$^+$, 860 (36) [M + H]$^+$, 665 (39) [M – ($Ph_2NC{\equiv}N$)]$^+$, 543 (8) [M – {L^2}$^-$ + H]$^+$. A single crystal of **4a** suitable for X-ray analysis was obtained by slow evaporation of a CH_2Cl_2/EtOH solution.

[ReO(L^{1a})(L^{2b})] (4b): $C_{30}H_{32}N_5O_4ReS_2$ (776.95): calcd. C 46.36, H 4.15, N 9.01, S 8.25; found C 46.27, H 4.03, N 8.85, S 8.28. IR (KBr): $\tilde{\nu}$ = 3055 (w), 2978 (w), 2924 (w), 2854 (w), 1527 (vs), 1488 (vs), 1427 (vs), 1359 (s), 1250 (vs), 1110 (s), 1026 (s), 964 (s), 771 (m), 694 (w) cm^{-1}. ^1H NMR (400 MHz, $CDCl_3$): δ = 1.23 (t, 3 H, CH_3), 1.25 (t, 3 H, CH_3), 3.80 (m, 2 H, NCH_2CH_3), 4.00 [m, 5 H, N-CH_2 (morph) + NCH_2CH_3], 4.02 [m, 1 H, N-CH_2 (morph)], 4.20 (m, 1 H, O-CH_2), 4.37 (m, 1 H, O-CH_2), 4.42 (m, 1 H, O-CH_2), 4.62 (m, 1 H, O-CH_2), 6.25 (t, J = 7.6 Hz, 1 H, PhOH), 6.38 (d, J = 7.9 Hz, 1 H, PhOH), 6.69 (t, J = 7.6 Hz, 1 H, PhOH), 6.91 (d, J = 8.0 Hz, 1 H, PhOH), 7.01 (t, J = 7.8 Hz, 2 H, Ph), 7.28 (m, 3 H, Ph), 7.30 (t, J = 7.3 Hz, 1 H, Ph), 7.53 (d, J = 8.2 Hz, 2 H, Ph), 7.57 (d, J = 7.2 Hz, 2 H, Ph) ppm. ^{13}C NMR (100 MHz, $CDCl_3$): δ = 13.43 (CH_3), 13.54 (CH_3), 47.25 (NCH_2), 47.37 (NCH_2), 48.36 (NCH_2), 49.97 (NCH_2), 67.25 (OCH_2), 67.74 (OCH_2), 117.14, 118.40, 120.95, 124.57, 127.52, 128.13, 129.47, 130.73, 130.86, 131.78, 135.58 and 135.64 (Ph), 145.36 (C_{ar}–N), 163.87 (C_{ar}–O), 171.04 (C=N, {L^{1a}}$^{2-}$), 172.01 (C=S, {L^{2b}}$^-$), 178.17 (C=S, {L^{1a}}$^{2-}$), 184.73 (C=O, {L^{2b}}$^-$) ppm. MS (FAB+): m/z (%) = 800 (15) [M + Na]$^+$, 778 (41) [M + H]$^+$, 691 (41) [M – morph]$^+$, 665 (45) [M – (morphC≡N)]$^+$, 543 (8) [M – {L^{2b}}$^-$ + H]$^+$.

[ReO(L^{1b})(L^{2b})] (4c): $C_{30}H_{30}N_5O_5ReS_2$ (790.93): calcd. C 45.56, H 3.80, N 8.86, S 8.10; found C 45.38, H 3.90, N 8.59, S 8.45. IR (KBr): $\tilde{\nu}$ = 3053 (w), 2970 (w), 2912 (w), 2855 (w), 1519 (vs), 1493 (vs), 1435 (vs), 1380 (s), 1353 (m), 1265 (s), 1250 (s), 1229 (s), 1115 (s), 1026 (s), 976 (s), 798 (m), 694 (w) cm^{-1}. ^1H NMR (400 MHz, $CDCl_3$): δ = 3.55 (m, 1 H, N-CH_2), 4.02–4.20 (m, 5 H, O-CH_2), 4.27 (m, 1 H, O-CH_2), 4.50 (m, 1 H, O-CH_2), 4.70 (m, 1 H, O-CH_2), 6.26 (t, J = 7.6 Hz, 1 H, PhOH), 6.41 (d, J = 7.9 Hz, 1 H, PhOH), 6.71 (t, J = 7.6 Hz, 1 H, PhOH), 6.92 (d, J = 7.9 Hz, 1 H, PhOH), 7.05 (t, J = 7.8 Hz, 2 H, Ph), 7.22 (m, 3 H, Ph), 7.31 (t, J = 7.3 Hz, 1 H, Ph), 7.55 (m, 4 H, Ph) ppm. ^{13}C NMR (100 MHz, $CDCl_3$): δ = 48.67 (NCH_2), 49.17 (NCH_2), 49.83 (NCH_2), 50.18 (NCH_2), 66.53 (OCH_2), 66.61 (OCH_2), 67.33 (OCH_2), 67.58 (OCH_2), 117.31, 118.60, 121.22, 125.03, 127.62, 128.19, 129.59, 130.88, 131.34, 131.96 and 135.54 (Ph), 145.91 (C_{ar}–N), 164.86 (C_{ar}–O), 171.40 (C=N, {L^{1b}}$^{2-}$), 172.16 (C=N,{L^{2b}}$^-$), 178.37 (C=S, {L^{1b}}$^{2-}$), 184.69 (C=O, {L^{2b}}$^-$) ppm.

[TcO(L^{1b})(L^{2b})] (5): Prepared by the procedures described above as path A (from **3** and HL^{1b}) and path C from (NBu_4)[$TcOCl_4$] and a mixture of H_2L^{1b} and HL^{2b}. In both procedures, a green solution was obtained. The solvent was removed under reduced pressure, and the residue was washed with cold MeOH to obtain a green solid. Single crystals were obtained by slow evaporation of an ace-

 © 2009 Wiley-VCH Verlag GmbH & Co. KGaA, Weinheim

Table 4. Crystal data and details of the structure determinations.

	3	**4a**·EtOH	**4b**	**5**	**6**
Formula	$C_{18}H_{17}ClN_3O_3STc$	$C_{40}H_{40}N_5O_4ReS_2$	$C_{30}H_{32}N_5O_4ReS_2$	$C_{30}H_{30}N_5O_5S_2Tc$	$C_{48}H_{45}N_5O_4PS_2Tc$
M_w	488.86	905.09	776.93	703.40	948.98
Crystal system	monoclinic	triclinic	triclinic	monoclinic	monoclinic
Space group	$P2_1/n$	$P\bar{1}$	$P\bar{1}$	$P2_1/c$	$P2_1/c$
a [Å]	10.342(1)	9.925(1)	10.646(1)	10.565(1)	15.973(3)
b [Å]	12.391(1)	12.322(1)	11.629(1)	33.082(3)	11.464(1)
c [Å]	15.173(2)	15.372(1)	13.541(1)	8.604(1)	23.687(5)
α [°]	90	81.78(1)	90.78(1)	90	90
β [°]	102.42(1)	85.96(1)	95.67(1)	97.89(1)	95.67(1)
γ [°]	90	85.26(1)	113.53(1)	90	90
V [Å^3]	1898.9(3)	1851.0(3)	1526.9(2)	2978.7(5)	4316(1)
Z	4	2	2	4	4
$D_{calcd.}$ [g cm^{-3}]	1.710	1.624	1.690	1.568	1.460
μ [mm^{-1}]	1.033	3.444	4.160	0.673	0.519
No. of reflections	6685	18640	27996	14209	34742
No. of independent	4929	9996	8144	6265	9157
No. parameters	277	469	379	418	551
R_1/wR_2	0.0633/0.0849	0.0642/0.0928	0.0252/0.0608	0.0529/0.0991	0.0873/0.1304
GOF	0.949	0.962	1.163	0.909	0.775

tone/CH_2Cl_2 solution. Yield: 86% (60 mg). $C_{30}H_{30}N_5O_5S_2Tc$ (703.63): calcd. Tc 14.1; found Tc 14.0. IR (KBr): $\tilde{\nu}$ = 3063 (w), 2962 (w), 2916 (w), 2854 (w), 1504 (vs), 1475 (m), 1435 (s), 1350 (s), 1265 (s), 1218 (s), 1111 (s), 1026 (s), 957 (s), 798 (m), 694 (m) cm^{-1}. ^{1}H NMR (400 MHz, $CDCl_3$): δ = 3.35 (m, 2 H, NCH_2), 3.72 (m, 2, NCH_2), 3.85 (m, 2 H, NCH_2), 3.98 (m, 3 H, NCH_2 + OCH_2), 4.1–4.3 (m, 4 H, OCH_2), 4.35 (m, 1 H, OCH_2), 4.53 (m, 1 H, OCH_2), 4.75 (m, 1 H, OCH_2), 6.36 (m, 2 H, PhOH), 6.81 (t, J = 7.5 Hz, 1 H, PhOH), 6.97 (d, J = 6.7 Hz, 1 H, PhOH), 7.09 (t, J = 7.1 Hz, 2 H, Ph), 7.23 (m, 3 H, Ph), 7.41 (t, J = 7.5 Hz, 1 H, Ph), 7.64 (m, 4 H, Ph) ppm.

[Tc(L^{1b})(L^{2b})(PPh$_3$)] (6): To a solution of **5** (70 mg, 0.1 mmol) in CH_2Cl_2 (10 mL) was added PPh_3 (131 mg, 0.5 mmol). The mixture was stirred at room temperature for 3 h, whereupon the colour changed from yellow green to red. The volume of the solvent was reduced to 2 mL and MeOH (3 mL) was added. Red crystals of the product were obtained by slow evaporation of this mixture. Yield: 89% (85 mg). $C_{48}H_{45}N_5O_4PS_2Tc$ (949.91): calcd. Tc 10.4; found Tc 10.5. IR (KBr): $\tilde{\nu}$ = 3051 (w), 2962 (w), 2843 (w), 1497 (vs), 1466 (vs), 1420 (vs), 1350 (s), 1265 (s), 1207 (s), 1119 (s), 1022 (s), 721 (w), 694 (m) cm^{-1}. Good-quality single crystals for X-ray diffraction were obtained by slow diffusion of *n*-hexane into a CH_2Cl_2 solution of **6**.

X-ray Crystallography: The intensities for the X-ray determinations were collected with a STOE IPDS 2T instrument with Mo-K_α radiation (λ = 0.71073 Å). Standard procedures were applied for data reduction and absorption correction. Structure solution and refinement were performed with SHELXS97 and SHELXL97.[24] Hydrogen atom positions were calculated for idealized positions and treated with the "riding model" option of SHELXL. A disorder was refined for the carbon atoms of the morpholinyl residue in compound **3**. Two parts share the N6 and O43 atoms with occupation percentage of 76/24%. More details on data collections and structure calculations are contained in Table 4. CCDC-725264 (for **3**), -725265 (for **4a**·EtOH), -725266 (for **4b**), -725267 (for **5**) and -725268 (for **6**) contain the supplementary crystallographic data for this paper. These data can be obtained free of charge from The Cambridge Crystallographic Data Centre via www.ccdc.cam.ac.uk/data_request/cif.

Supporting Information (see footnote on the first page of this article): NMR spectra of compounds **4a** and **4b**.

Acknowledgments

We gratefully acknowledge grants from the Government of Vietnam, the DAAD (Germany) and CAPES (Brazil).

[1] a) S. Banerjee, M. R. A. Pillai, N. Ramamoorthy, *Semin. Nucl. Med.* **2001**, *31*, 260–277; b) J. R. Dilworth, S. Parrott, *Chem. Soc. Rev.* **1998**, *27*, 43–55.
[2] a) P. A. Schubiger, R. Alberto, A. Smith, *Bioconjugate Chem.* **1996**, *7*, 165–179; b) J. P. DiZio, R. Fiaschi, A. Davison, A. G. Jones, J. A. Katzenellenbogen, *Bioconjugate Chem.* **1991**, *2*, 353–366.
[3] a) J. Le Gal, F. Tisato, G. Bandoli, M. Gressier, J. Jaud, S. Michaud, M. Dartiguenave, E. Benoist, *Dalton Trans.* **2005**, *23*, 3800–3807; b) H. P. Vanbilloen, G. M. Bormans, M. J. De Roo, A. M. Verbruggen, *Nucl. Med. Biol.* **1995**, *22*, 325–338; c) T. N. Rao, D. Adhikesavalu, A. Camerman, A. R. Fritzberg, *J. Am. Chem. Soc.* **1990**, *112*, 5798–5804.
[4] S. S. Jurisson, J. D. Luxdon, *Chem. Rev.* **1999**, *99*, 2205–2218.
[5] a) J. Giglio, A. Rey, H. Cerecetto, I. Pirmettis, M. Papadopoulos, E. Leon, A. Monge, A. Lopez de Cerain, A. Azqueta, M. Gonzalez, M. Fernandez, A. Paolino, A. Leon, *Eur. J. Med. Chem.* **2006**, *41*, 1144–1152; b) X. Chen, F. J. Femia, J. W. Babich, J. Zubieta, *Inorg. Chim. Acta* **2000**, *307*, 88–96; c) K. P. Maresca, F. J. Femia, G. H. Bonavia, J. W. Babich, J. Zubieta, *Inorg. Chim. Acta* **2000**, *297*, 98–105.
[6] a) B. Nock, T. Maina, D. Yannoukakos, I. C. Pirmettis, M. S. Papadopoulos, E. Chiotellis, *J. Med. Chem.* **1999**, *42*, 1066–1075; b) R. Syhre, S. Seifert, H. Spies, A. Gupta, B. Johannsen, *Eur. J. Nucl. Med.* **1998**, *25*, 793–796.
[7] B. Nock, T. Maina, F. Tisato, M. Papadopoulos, C. P. Raptopoulou, A. Terzis, E. Chiotellis, *Inorg. Chem.* **1999**, *38*, 4197–4202.
[8] X. Chen, F. J. Femia, J. W. Babich, J. Zubieta, *Inorg. Chim. Acta* **2000**, *308*, 80–90.
[9] a) D. Papagiannopoulou, I. Pirmettis, M. Pelecanou, D. Komiotis, M. Sagnou, D. Benaki, C. Raptopoulou, A. Terzis, M. S. Papadopoulos, *Inorg. Chim. Acta* **2007**, *360*, 3597–3602; b) A. Chiotellis, C. Tsoukalas, M. Pelecanou, A. Papadopoulos, C. Raptopoulou, A. Terzis, I. Pirmettis, M. Papadopoulos, E. Chiotellis, *Inorg. Chem.* **2006**, *45*, 5635–5640.
[10] T. I. A. Gerber, P. Mayer, Z. R. Tshentu, *J. Coord. Chem.* **2005**, *58*, 947–953.
[11] F. Mevellec, A. Roucoux, N. Noiret, H. Patin, *Inorg. Chim. Acta* **2002**, *332*, 30–36.

 © 2009 Wiley-VCH Verlag GmbH & Co. KGaA, Weinheim

[12] C. Bolzati, M. Porchia, G. Bandoli, A. Boschi, E. Malago, L. Uccelli, *Inorg. Chim. Acta* **2001**, *315*, 205–212.
[13] H. H. Nguyen, J. Grewe, J. Schroer, B. Kuhn, U. Abram, *Inorg. Chem.* **2008**, *47*, 5136–5144.
[14] a) H. H. Nguyen, U. Abram, *Inorg. Chem.* **2007**, *46*, 5310–5319; b) H. H. Nguyen, U. Abram, *Z. Anorg. Allg. Chem.* **2008**, *634*, 1560–1564.
[15] a) L. Hansen, X. Xu, M. Lipowska, A. Taylor Jr, L. G. Marzilli, *Inorg. Chem.* **1999**, *38*, 2890–2897; b) J. P. O'Neil, S. R. Wilson, J. A. Katzenellenbogen, *Inorg. Chem.* **1994**, *33*, 319–323.
[16] R. Alberto, "Technetium" in *Comprehensive Coordination Chemistry II* (Eds.: J. A. McCleverty, T. J. Mayer), Elsevier, Amsterdam, **2003**, vol. 5, pp. 127–270.
[17] U. Abram, "Rhenium" in *Comprehensive Coordination Chemistry II* (Eds.: J. A. McCleverty, T. J. Mayer), Elsevier, Amsterdam, **2003**, vol. 5, pp. 271–402.
[18] a) S. Abram, U. Abram, E. Schulz Lang, J. Strähle, *Acta Crystallogr., Sect. C* **1995**, *51*, 1078–1080 and references cited therein; b) A. Paulo, A. Domingos, J. Marcalo, A. Pires de Matos, I. Santos, *Inorg. Chem.* **1995**, *34*, 2113–2120; c) H. Braband, O. Blatt, U. Abram, *Z. Anorg. Allg. Chem.* **2006**, *632*, 2251–2255.
[19] a) R. Alberto, R. Schibli, A. Egli, P. A. Schubiger, W. A. Herrmann, G. Artus, U. Abram, T. A. Kaden, *J. Organomet. Chem.* **1995**, *493*, 119–127; b) N. P. Johnson, C. J. L. Lock, G. Wilkinson, *Inorg. Synth.* **1967**, *9*, 145–148.
[20] R. W. Thomas, A. Davison, H. S. Trop, E. Deutsch, *Inorg. Chem.* **1980**, *19*, 2840–2842.
[21] J. Chatt, G. A. Rowe, *J. Chem. Soc.* **1962**, 4019–4033.
[22] L. Beyer, R. Widera, *Tetrahedron Lett.* **1982**, *23*, 1881–1882.
[23] H. Hartmann, L. Beyer, E. Hoyer, *J. Prakt. Chem.* **1978**, *320*, 647–650.
[24] G. M. Sheldrick, *SHELXS-97 and SHELXL-97, Programs for the Solution and Refinement of Crystal Structures*, University of Göttingen, Göttingen, Germany, **1997**.
[25] L. J. Farrugia, *J. Appl. Crystallogr.* **1997**, *30*, 565–566.

Received: March 28, 2009
Published Online: June 17, 2009

 © 2009 Wiley-VCH Verlag GmbH & Co. KGaA, Weinheim